Measurement of the neutron-induced fission cross-section of ^{240,242}Pu

P. Salvador-Castiñeira,[a,b] F-J. Hambsch,[a] T. Bryś,[a] S. Oberstedt,[a] C. Pretel[b], M. Vidali[a]
[a]European Commission, JRC-IRMM, Geel, Belgium
[b]Institute of Energy Technologies, Technical University of Catalonia, Barcelona, Spain

Abstract

Fast spectrum neutron-induced fission cross-section data for transuranic isotopes are in high demand in the nuclear data community. In particular, highly accurate data are needed for the new Generation-IV nuclear applications. The aim is to obtain precise neutron-induced fission cross-sections for ^{240}Pu and ^{242}Pu. In this context accurate data on spontaneous fission half-lives have also been measured. To minimise the total uncertainty on the fission cross-sections the detector efficiency has been studied in detail. Both isotopes have been measured using a twin Frisch-grid ionisation chamber (TFGIC) due to its superiority compared to other detector systems in view of radiation hardness, $2 \times 2\pi$ solid angle coverage and very good energy resolution.

Introduction

In a recent assessment of target accuracies and uncertainties the OECD Nuclear Energy Agency (NEA) highlighted the need for improved nuclear data to be used in model calculations for innovative reactor systems (GEN-IV) (Salvatores, 2008). In this paper the neutron-induced fission cross-sections of ^{240,242}Pu have been identified as of highest priority for fast neutron spectrum reactors. Their target uncertainties are very stringent and are requested to be 1-2% for ^{240}Pu and 3-5% for ^{242}Pu from current uncertainties of 6% and 20%, respectively.

In the framework of the Accurate Nuclear Data for Nuclear Energy Sustainability (ANDES) collaboration, several actinides are being studied, among them ^{240,242}Pu. Different experimental methods are being used to determine their neutron-induced fission cross-section. For the first time the new digital data acquisition technique has been applied for cross-section measurements. Using digital electronics and storing the full waveform opens up new analysis possibilities not available using regular analogue electronics.

This report gives an overview of the present status of the experiment in terms of newly determined spontaneous fission half-lives for both ^{240,242}Pu and the resulting preliminary fission cross-sections.

Experimental set-up

A twin Frisch-grid ionisation chamber (TFGIC) has been chosen as fission fragment (FF) detector. Its characteristics (radiation resistance, solid angle of nearly $2 \times 2\pi$ and good

energy resolution) made this type of detector the excellent choice for performing direct kinematics fission experiments.

A schematic representation of the set-up is presented in Figure 1. Since the two samples used in this study have a thick backing, allowing to detect just one FF, they were placed in back-to-back geometry. The TFGIC was filled with P10 (90% Ar + 10% CH_4) as counting gas at a pressure of 1 052 mbar with a constant flow of ~50 ml/min. The cathode-grid distance was 31 mm and the grid-anode distance was 6 mm, allowing the FF to be fully stopped within the space between the cathode and the grid. The cathode was common for the two samples and was set at a high voltage (HV) of -1.5 kV, while the two anodes were set at 1 kV. Both grids were grounded. Grids and anodes were connected to charge-sensitive pre-amplifiers, and the output was fed into a 12 bit 100 MHz waveform digitiser (WFD). The cathode was connected to a current-sensitive pre-amplifier. The output signal was split, one signal was fed into the WFD and the other was treated with a timing filter amplifier (TFA) and a constant fraction discriminator (CFD) resulting the trigger signal for all the WFD.

The Pu samples used in this experiment were produced by the so-called molecular plating technique in the target preparation laboratory of the JRC-IRMM. Due to the short α half-life of the ^{240}Pu, 6 561 yr (0.1%), the sample has a total mass of only 92.9 μg (0.4%) with an α-activity of 0.8 MBq (0.4%). The ^{24}2Pu has an α half-life longer than 105 yr, for this reason more material could be deposited on top of the disk, being its mass of 671 μg (0.9%) and its α-activity of 0.1 MBq (0.3%). The main contribution on the mass uncertainty of ^{242}Pu is due to its α half-life and its uncertainty, 3.75 × 105 yr (0.5%). The activity of both samples was determined by defined solid angle α-particle counting. The purity of the samples is higher than 99.8% and their atomic abundances were measured by mass spectrometry. The main characteristics of the ^{240,242}Pu samples are summarised in Table 1 (Sibbens, *et al.*, 2013).

The experiments were performed at the Van de Graaf (VdG) accelerator at JRC-IRMM. The neutron-producing reactions used were ^{7}Li(p,n)^{7}Be and T(p,n)^{3}He, giving a neutron energy range from 0.2 MeV to 3 MeV. The reference samples used are described in Table 2.

Figure 1

(a) Schematic drawing of a twin Frisch-grid ionisation chamber (TFGIC) with a reference sample in one side and a sample under study in the other

(b) Scheme of the electronics for one chamber side

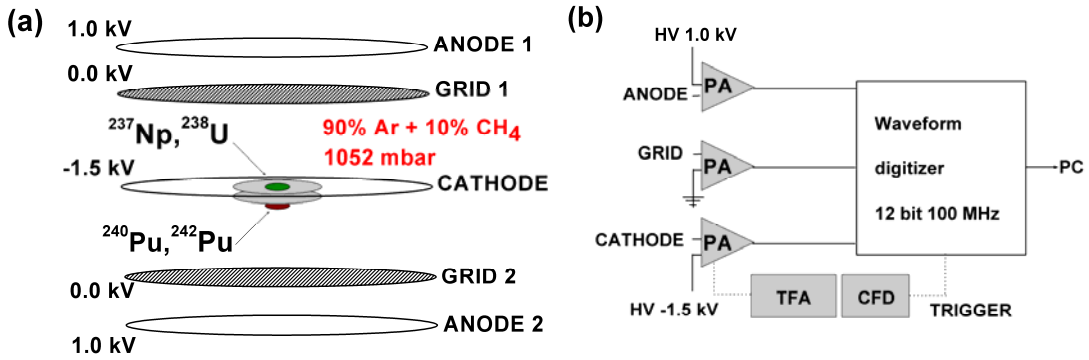

Table 1: Main characteristics of the ^{240,242}Pu samples

All the uncertainties are expanded with a coverage factor k = 1;
the expanded uncertainty of the sample purity has a coverage factor of k = 2

	^{240}Pu	^{242}Pu
Method	Molecular plating	Molecular plating
Chemical composition (assumed)	$Pu(OH)_4$	$Pu(OH)_4$
Total mass (μg) (calculated)	119.22 (0.4%)	859.54 (0.9%)
Total area density (μg/cm^2) (calculated)	16.9 (0.4%)	122 (0.8%)
Backing	Aluminium	Aluminium
Mass (μg)	92.9 (0.4%)	671 (0.9%)
Areal density (μg/cm^2)	13.19 (0.4%)	95.3 (0.8%)
α-activity (MBq)	0.780 (0.4%)	0.0984 (0.3%)
Purity	99.8915(*18*)%	99.96518(*45*)%

Source: Sibbens, *et al*. (2013).

Table 2: Main characteristics of the secondary standards used

	^{237}Np	^{238}U
Mass (μg)	391.3 (0.3%)	614 (0.5%)
Areal density (μg/cm^2)	308.1	86.9
α-activity (Bq)	10168 (0.1%)	7.64 (0.5%)

Source: Pommé (2012).

Data analysis

Several corrections have been applied to the raw anode and grid signals: α pile-up correction, grid inefficiency, etc. A detailed description is given in (Salvador-Castiñeira, *et al.*, 2013). To determine the detection efficiency of the ionisation chamber the procedure described by Budtz-Jørgensen and Knitter (1984) has been used based on the following equation to determine the total number of emitted FF (N_{cos}):

$$N_{\cos} = A + \Delta A \tag{1}$$

with A being the integral of the cosine distribution and ΔA the missing part related with the thickness of the sample [Figure 2(a)]. To extract the sample loss the anode *PH* distribution (N_{PH}) must be considered and extrapolated down to 0 (ΔN_{PH}) to account for FF emitted but not detected due to the high electronic threshold requested not to trigger on α events [Figure 2(b)]. The experimental efficiency due to sample loss ($\in_{\exp}$) will then be calculated as:

$$\in_{\exp} = \frac{N_{PH} + \Delta N_{PH}}{N_{\cos}} = \frac{N_{2\pi}}{N_{\cos}} \tag{2}$$

During the analysis of the P10 data we found a strong correlation between the degradation of the cosine distribution and the α-activity of the sample, obtaining a lower efficiency for the thinner but more active target (^{240}Pu) and a higher one for the thicker

Figure 2

(a) Angular distribution for ^{242}Pu. The FF loss inside the sample is visible at low cos θ values. By determining the integral of the distribution and ΔA (the missing part of the distribution) one can obtain the sample loss.

(b) PH distribution for ^{242}Pu and determination of counts under the electronic threshold

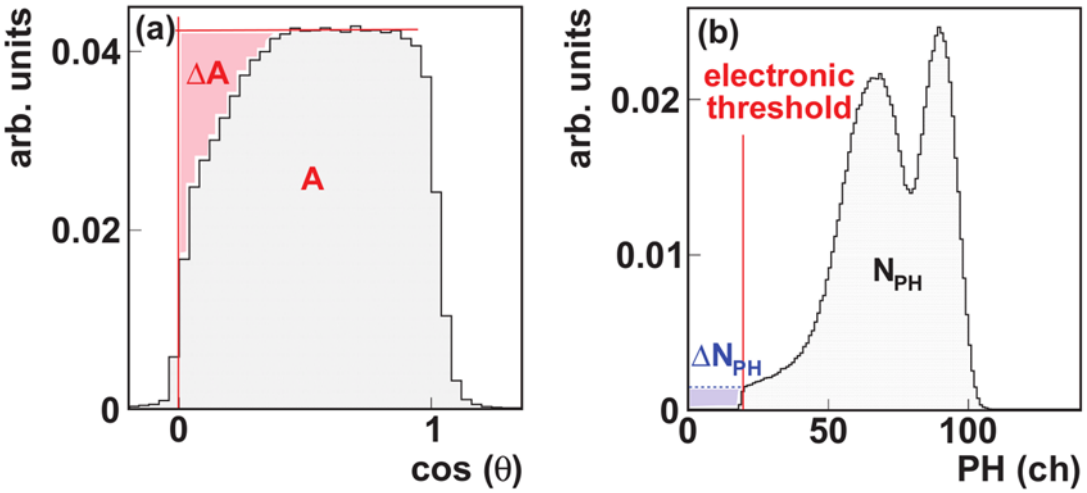

but less active target (^{242}Pu). Improving the signal rise time by using CH_4 as counting gas, which has a drift velocity two times higher than P10 (Knoll, 2000), the results on the efficiency calculation of the ionisation chamber also improved, getting closer to what should be expected with theoretical calculations. To verify the efficiency results obtained with the different analysis methods, theoretical calculations using SRIM (Ziegler, Biersack and Ziegler, 2008) stopping power ranges and Geant4 simulations (2014) have been performed as well.

The theoretical calculation has been done as presented by Salvador-Castiñeira, *et al.* (2013). Properties for two typical FF have been used. The loss inside the sample can be calculated as:

$$\Delta_{sample} = \frac{t}{2R_{sample}} = \frac{t}{2}\sum_i \frac{W_i}{R_i} \tag{3}$$

with t as the thickness of the sample, R_i the range of isotope i and W_i the weight fraction of isotope i in the sample.

Simulations with Geant4 have been performed with a FF kinetic energy distribution obtained with the GEF code (Schmidt and Jurado, n.d.). The transmitted FF from the sample to the counting gas were obtained from the simulations.

Spontaneous fission half-life

The SF half-life has been calculated using:

$$T_{1/2,SF} = \frac{\%^j Pu}{A_j} \cdot \frac{1}{\left(\frac{C_{SF}}{t \cdot \in_j \cdot \ln 2 \cdot m_{Pu} \cdot N_A} - \sum_i^n \frac{\%^i Pu}{A_i \cdot T_{1/2,SF}(i)} \right)} \tag{4}$$

where $\%^{j}Pu$ is the purity of the sample, A_j its atomic mass, C_{SF} the counts detected, $\in_j$ the detection efficiency, m_{Pu} the sample mass, N_A the Avogadro's number and $\sum_i^n \frac{\%^{i}Pu}{A_i \cdot T_{1/2,SF}(i)}$ the contribution from the other isotopes contained in the sample.

Several measurements have been performed with each sample. Figure 3 summarises in a graph the resulting $T_{1/2,SF}$ values. Run 1 for ^{240}Pu and 1-5 for ^{242}Pu were performed with P10 as counting gas, while runs 2-3 for ^{240}Pu and 6-7 for ^{242}Pu with CH_4. Each run contains several individual data sets with up to 250 000 fission events using P10 and up to 1 500 000 events using CH_4. All labelled runs are performed using a different electronic threshold. The error bars in the plot describe the statistical and the systematic uncertainties, the thick horizontal line is an eye guide for the weighted average of our data and the dotted lines are the final uncertainties (systematic and statistical) expressed with 1σ. The bullet symbols represent previous experimental results, the highlighted literature value is a weighted average of a subset of the literature data made by Holden and Hoffman (2000) and using the same data by reference Chechev (2005)/LNHB (n.d.). Table 3 lists the present uncertainty budget and Table 4 lists the weighted average of our experimental data together with the weighted average of the literature values by Holden and Hoffman (2000) and the same weighted average calculated by Chechev (2005)/LNHB (n.d.).

Figure 3: SF half-life results for ^{240}Pu (a) and ^{242}Pu (b) (stars) compared with some literature values (bullets), their weighted average calculated by Holden and Hoffman (2000) and the weighted average calculated by Chechev (2005)/LNHB (n.d.)

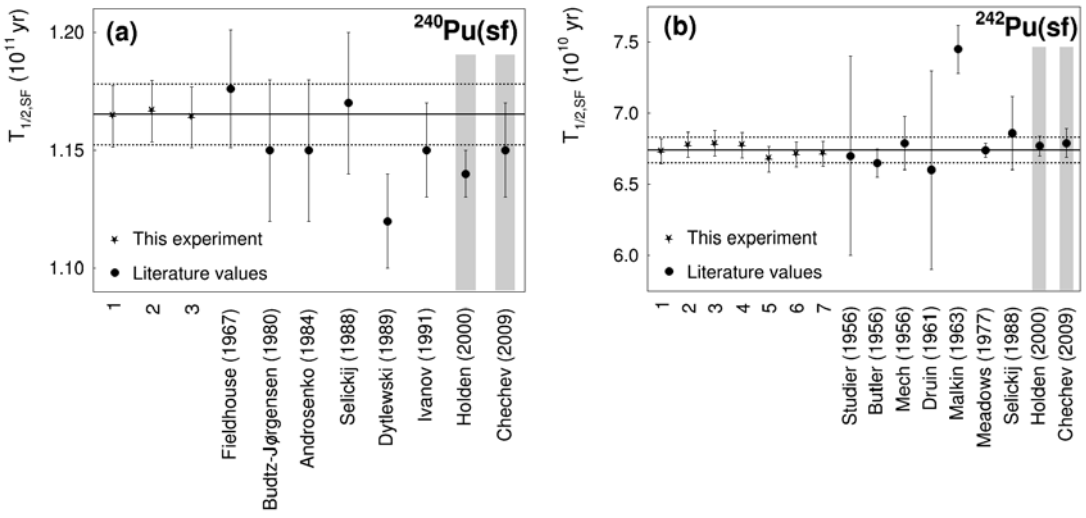

Table 3: Summary of the uncertainties corresponding to the SF half-life ($T_{1/2,SF}$) for ^{240,242}Pu

Uncertainty source	^{240}Pu	^{242}Pu
Statistical	0.13%	< 0.1%
Mass	0.4%	0.9%
Sample efficiency	1%	1%
Sample purity	< 0.001%	< 0.001%
Dead time acquisition system	< 0.07%	< 0.12%
Total (systematic and statistical)	1.1%	1.3%

Table 4: Summary of the SF half-life ($T_{1/2,SF}$) for ^{240,242}Pu

The experimental uncertainties presented are both the statistical and systematic. The weighted average of literature values presented by Holden and Hoffman (2000) and that calculated by Chechev (2005)/LNHB (n.d.) using the same literature data.

$T_{1/2,SF}$ (yr)	^{240}Pu	^{242}Pu
Holden and Hoffman (2000)	1.14×10^{11} (0.9%)	6.77×10^{10} (1.0%)
Chechev (2005)/LNHB (n.d.)	1.15×10^{11} (1.7%)	6.79×10^{10} (1.4%)
This experiment	1.165×10^{11} (1.1%)	6.74×10^{10} (1.3%)

Our results are in agreement with the literature values for ^{242}Pu. Nevertheless, and using exactly the same method, the ^{240}Pu SF half-life is slightly higher than some of the literature values. This could be explained by the high α-activity of the sample. By having a more precise discrimination of α-particle signals our count rate might have been lower than in previous experiments done with analogue electronics, thus obtaining a higher SF half-life value. More details are given in Salvador-Castiñeira, *et al.* (2013).

Fission cross-sections

Measurements have been performed at the Van de Graaff facility of the JRC-IRMM. Several campaigns have been done for the two plutonium isotopes using the two different standards. The neutron-producing reactions used were ^{7}LiF(p,n)^{7}Be for neutron energies between 0.2 MeV and 1.8 MeV and using ^{237}Np(n,f) as a reference; and T(p,n)^{3}He for neutron energies between 1.8 and 3 MeV and using ^{238}U(n,f) as a reference. Based on the newly determined half-lives and efficiency determination of the ionisation chamber the fission cross-sections have been calculated for both ^{240}Pu and ^{242}Pu according to the following equation:

$$\sigma_{Pu}(E_0) = \left[\frac{N_{ref}}{N_{Pu}} \cdot \frac{(C_{Pu}/\in_{Pu} - C_{SF})}{C_{ref}/\in_{ref}} - \sum_i P_i \frac{\sigma_i(E_0)}{\sigma_{ref}(E_0)} \right] \cdot \left(\frac{\phi_0^{ref}}{\phi_0^{Pu}} \cdot \sigma_{ref}(E_0) + \frac{\phi_1^{ref}}{\phi_0^{Pu}} \cdot \sigma_{ref}(E_1) \right) - \frac{\phi_1^{Pu}}{\phi_0^{Pu}} \cdot \sigma_{Pu}(E_1) \quad (5)$$

where E_0 and E_1 refer to the ground state and the first excited state of the ^{7}Li(p,n)^{7}Be reaction, respectively; ϕ_0 is the flux related to the ground state of the Li reaction and ϕ_1 to the excited state of the same reaction; N_i are the number of atoms in the sample i, C_i are the number of counts detected from the sample i, C_{SF} are the number of spontaneous fission counts from the plutonium sample, $\in_i$ is the transmission probability of a fission fragment (FF) to leave the sample and enter into the counting gas, $\sum_i P_i \frac{\sigma_i(E_0)}{\sigma_{ref}(E_0)}$ is the contribution on the plutonium fission counts from the impurities of the sample and $\sigma_{ref}(E_i)$ is the cross-section from the reference isotope. When the T(p,n)^{3}He reaction was used, thus the ^{238}U sample, Eq. (5) was simplified since the neutron-producing reaction gave a quasi-monoenergetic beam. The excited state of the Li reaction grows its influence with the increasing neutron energy; being about 8% of the total neutron flux at 1.8 MeV (ground state energy).

The provisional results are given in Figure 4, for ^{240}Pu and for ^{242}Pu.

Figure 4: Neutron-induced fission cross-section of ^{240}Pu (left) and ^{242}Pu (right)

The triangles represent our data taken relative to the ENDF/B-VII.1 ^{237}Np evaluation; while the bullets are data taken relative to the ENDF/B-VII.1 ^{238}U evaluation

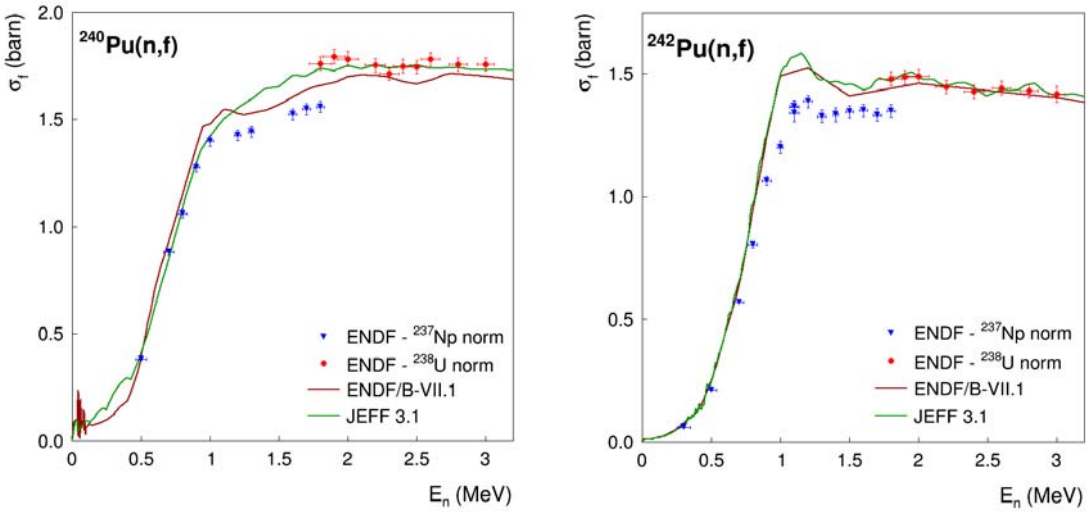

Two different normalisations have been performed. At first, the data were normalised to the ENDF/B.VII.1 evaluation (Chadwick, *et al.*, 2011) for the two reference isotopes (^{237}Np – blue symbols; ^{238}U – red symbols). A clear discrepancy between the data relative to the ^{237}Np evaluation and the ^{238}U evaluation is observed. The difference at the overlapping incident neutron energy point (at 1.8 MeV) amounts to about 13% in both cases. The data for both ^{240}Pu and ^{242}Pu measured relative to the ^{238}U fission cross-section is in agreement with the JEFF-3.1 evaluation. The threshold for ^{240}Pu is very well reproduced and also agrees best with the JEFF-3.1 evaluation. There is a distinct difference above threshold for both Pu isotopes if the ^{237}Np ENDF/B-VII.1 evaluation is used.

The uncertainty calculation includes the contribution of the sample mass, the uncertainties on half-life and isotope content, statistics and efficiency. When normalising to ^{238}U the uncertainty budget considered includes, in addition, the uncertainty of the reference cross-section; in that particular case the value is around 0.7% in the considered energy range. The uncertainty that should be considered when using the cross-section of ^{237}Np as a reference amounts from 3.5 to 5% from 0.2 MeV up to 1.8 MeV. In the case of ^{237}Np, this source of uncertainty is not yet added in the present results.

Recently, new values for the neutron-induced fission cross-section for ^{237}Np were published by Paradela, *et al.* (2010), these data were around 5% higher in value than the current evaluations (see Figure 5). By normalising our ^{237}Np data to Paradela, *et al.* (2010), the green symbols would be obtained in Figure 6. Then in case of ^{240}Pu the new results would be much better in agreement with the ENDF/B-VII.1 evaluation over the whole energy range covered by the ^{237}Np reference. For ^{242}Pu however, both the threshold and above threshold values are still too small compared to the ENDF/B-VII.1 evaluation. The difference in the overlap region to the ^{238}U reference data is in both cases still 5-8%.

Conclusions

The neutron-induced fission cross-section has been measured for ^{240,242}Pu at the Van de Graaff facility of the JRC-IRMM. The energy range studied has been between 0.2 MeV and 3 MeV neutron incoming energy. Two different secondary standards have been used: ^{237}Np and ^{238}U. The results obtained at the overlap neutron energy region for the two standards used (1.8 MeV) do not agree within uncertainties. The preliminary

results presented in Figures 2-4 neither agree with each other nor with evaluations. All points to a too-small ^{237}Np fission cross-section. New measurement of this cross-section by Paradela, *et al.* (2010) are 5% larger compared to the present evaluation but are still too small to make the match in the overlap region between the two standards.

Figure 5

Left: Ratio of the neutron-induced fission cross-section of ^{237}Np and the ^{235}U; three groups of data are distinguished

Right: Neutron-induced fission cross-section of ^{237}Np; the latest evaluations are shown together with data from Paradela, *et al.* (2010) and Jiacoletti, Brown and Olson (1972)

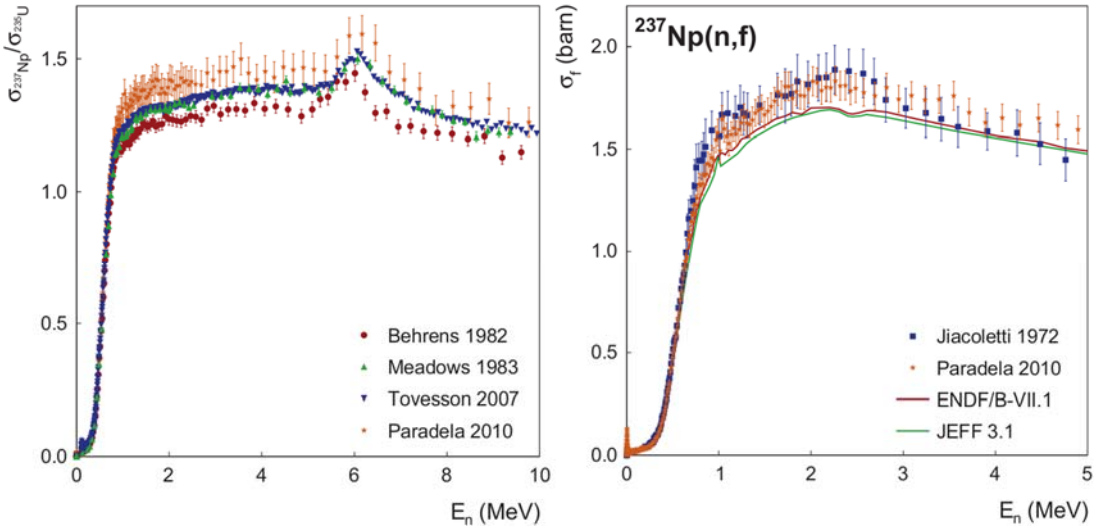

Figure 6: Neutron-induced fission cross-section of ^{240}Pu (left) and ^{242}Pu (right)

The blue triangles represent our data taken relative to the ENDF/B-VII.1 ^{237}Np evaluation, while the bullets are data taken relative to the ENDF/B-VII.1 ^{238}U evaluation; a new normalisation of the ^{237}Np data is presented relative to the new cross-section values of Paradela, *et al.* (2010)

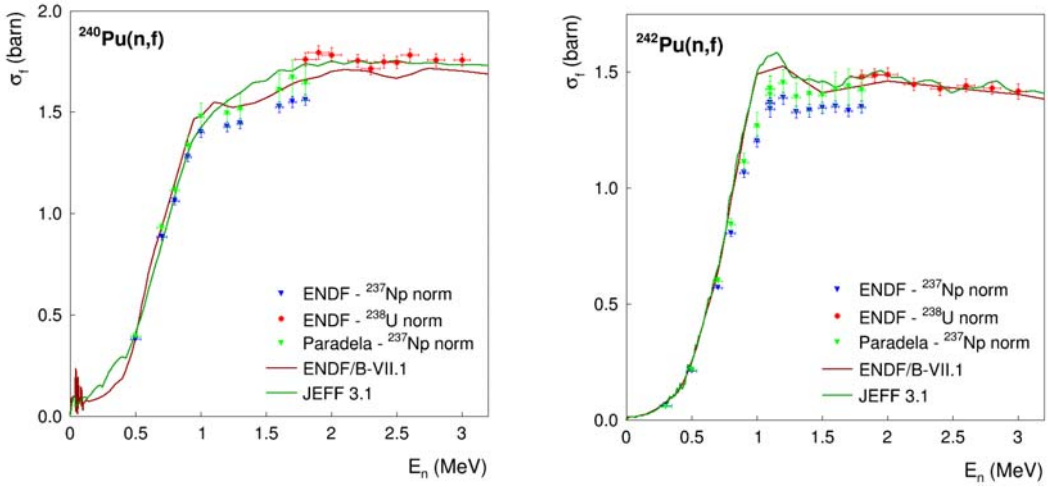

Acknowledgements

One of the authors (P.S-C.) acknowledges financial support from the ANDES collaboration (contract No. FP7-249671).

References

Budtz-Jørgensen, C. and H-H. Knitter (1984), *Nucl. Sci. Eng.*, 86, pp. 10-21.

Chadwick, M.B., *et al.* (2011), "ENDF/B-VII.1 Nuclear Data for Science and Technology: Cross Sections, Covariances, Fission Product Yields and Decay Data", *Nucl. Data Sheets*, 112, p. 2887.

Chechev, V.P. (2005), *Proc. Intern. Conf. Nuclear Data for Science and Technology*, Santa Fe, New Mexico, 26 September-1 October 2004, R.C. Haight, *et al.* (eds.), Vol. 1, p. 91, AIP Conf. Proc., 769.

Geant4 (2014), Geant4 website, accessed 23 June 2014, http://geant4.web.cern.ch/geant4/.

Holden, N.E. and D.C. Hoffman (2000), *Pure Appl. Chem.*, 72, pp. 1525-1562.

Jiacoletti, R.J., W.K. Brown and H.G. Olson (1972), *Fission Cross Sections of ^{237}Np from 20 eV to 7 MeV Determined from a Nuclear-Explosive Experiment*, Los Alamos National Laboratory (LANL), Los Alamos, NM, United States.

Knoll, G.F. (2000), *Radiation Detection and Measurement*, John Wiley and Sons, Inc., New York, United States, 3rd edition.

LNHB (Laboratoire National Henri Becquerel) (n.d.), "Recommended Data" webpage on LNHB website, accessed 23 June 2014, www.nucleide.org/DDEP_WG/DDEPdata_by_Z.htm.

Paradela, C., *et al.* (2010), "Neutron-Induced Fission Cross Section of ^{234}U and ^{237}Np Measured at the CERN Neutron Time-of-Flight (n_TOF) Facility", *Physical Review C*, 82 (3), 034601.

Pommé, S. (2012), private communication.

Salvador-Castiñeira, P., *et al.* (2013), "Highly Accurate Measurements of the Spontaneous Fission Half-Life of ^{240,242}Pu", forthcoming in *Phys. Rev. C*.

Salvatores, M. (2008), *Uncertainty and Target Accuracy Assessment for Innovative Systems Using Recent Covariance Data Evaluations*, NEA/WPEC-26, OECD/NEA, Paris.

Schmidt, K-H. and B. Jurado (n.d.), "GEF-code Version 2012/2.7", webpage on Centre d'Etudes Nucléaires de Bordeaux Gradignan (CENBG) website, accessed 23 June 2014, www.cenbg.in2p3.fr/-GEF-.

Sibbens, G., *et al.* (2013), "Preparation of ^{240}Pu and ^{242}Pu Targets to Improve Cross Section Measurements for Advanced Reactors and Fuel Cycles", *J. Rad. Nucl. Chem.*, 297:DOI 10.1007/s10967–013–2669–6.

Ziegler, J.F., J.P. Biersack and M.D. Ziegler (2008), *SRIM – The Stopping and Range of Ions in Matter*, SRIM Co., Chester, MD, United States, ISBN 0-9654207-1-X, www.srim.org.